International Journal of Enhanced Research in Science Technology & Engineering, ISSN: 2319-7463
Vol. 3 Issue 7, July-2014, pp: (75-88), Impact Factor: 1.252, Available online at: www.erpublications.com

Preparation and Characterization of YTTRIA Stabilized Zirconia (8YSZ) Nanofiber for Medical Application

Amit Biswas[1], Niladri Panda[2], Pravin Bhattarai[*3]
[123]Department of Biotechnology & Medical Engineering, National Institute of Technology, Rourkela, Orissa, India

Abstract: A simple and inexpensive electrospinning technique was used to synthesize 8 mol% yttria-stabilized zirconia (8YSZ) ceramic nanofibers having average diameter of ~200 nm after calcination. As-spun nanofibers after subjected to pre-selected time-temperature calcination profile retained excellent fiber morphology and were phase transformed, enhancing its further applicability in medical field. The characterization techniques such as Scanning electron microscopy (SEM), X-ray diffraction (XRD), Fourier transform infrared spectroscopy (FTIR) and Energy dispersive spectroscopy (EDS) were selected for the evaluation of morphological and crystallinity properties of as-spun and processed ceramic nanofibers whereas, MTT and haemolytic assay were implemented to determine the biological characteristics, e.g. invitro biocompatibility of the fabricated material. It is believed that such processed ceramic nanofibers retaining its phase and morphological properties and possessing least cytotoxicity can have great application in the medical field.

Introduction

One aspect of present issues and great importance to the basic understanding of the performance of materials on their optical, chemical and mechanical properties is by the virtue of its size and dimension for real time application in manifold devices[1].In this regard, study of one-dimensional materials has increased significantly in various research institutes all over the world. Materials or structures having at least one of its dimension 100 nm or less are considered as one-dimensional materials. The novel chemical, physical and biological properties of one-dimensional materials can be attributed to its unique shape and nanofibrous morphology that can be easily deployed in optics, catalysis, data storage devices and biological scaffolds. Inadequacy of such properties in bulk materials where the particle is in the size of micron level further enhances study and use of one-dimensional materials. Currently, the present need marks the possibility of application of such attributes in nano-sized inorganic materials as quantum dots in a host device, e.g. MEMs, sensors, structural component in artificial organs and arteries, reinforced composites, electrodes, photocatalysts.Hence, there is still a lot of opportunities in the development of nanoarchitectured ceramics that can be exploited for its use as high performance devices, tissue engineering scaffolds and a lot more.

Electrospinning is most widely chosen tool for synthesizing one-dimensional(1D)nanostructures which include ribbons, fibers, filled and hollow tubes from the fact that it's quite simple, easy to use and relatively inexpensive technique. The unique features of such as-spun nanofibers are one-dimensional morphology, extraordinary length, large surface area and highly porous structures[2, 3].In this work, a simple electrospinning technique was used to fabricate 8 mol% yttria stabilized zirconia nanofiber from PVP/YSZ. A composite solution (sol) of starting materials were prepared and electrospun in different environmental conditions. Such, as-prepared scaffolds were subsequently processed to obtain the desired ceramic composition. The various morphological and phase transformations likely to occur at this transition phase was verified by different characterization tools as described later. The vital property of a material for medical application, biocompatibility was investigated by MTT and Haemolytic assay.

2. Experimental Procedure

2.1Preparation of the solutions

High purity zirconyloxychlorideoctahydrate, $ZrOCl_2.8H_2O$ (purity 98%, MW 322.25) was procured from Chemika-Biochemika Reagents, while yttrium oxide, Y_2O_3 (purity 99.9%, MW 225.81) from LobaChemie, was used as the precursors for the synthesis of the YSZ fibers.

Two categories of 8 mole% YSZ sol were prepared in this experimental work. To achieve 8YSZ sol (I), the 0.8 g Y_2O_3 was first converted to yttrium nitrate by dissolving in concentrated nitric acid. Initially, 2 ml of concentrated nitric acid was pipetted and transferred to a 5 ml beaker in which earlier weighed 0.8 g Y_2O_3 was added. The solution was then left for continuous magnetic stirring under mild heat until the excess of nitric acid was evaporated and solution was clear. 12.15 g $ZrOCl_2.8H_2O$ was dissolved into 10 ml deionized water and then added to the yttrium nitrate solution followed by continuous stirring. While to achieve 8YSZ sol (II), 0.0226 gm of yttrium oxide (Y_2O_3) and 0.0177 gm, 0.17 gm and 0.26 gm of zirconium oxychloride were dissolved separately in 10 ml of deionized water to give 0.01 M, 0.1 M and 0.15 M of stock solution respectively. Later, 9.2 ml of zirconium and 0.8 ml of yttrium solution were mixed together and left for constant stirring. 5 ml of above prepared yttrium-zirconium solution was dissolved in 15 wt% of PVP (0.7 gm in 5 ml of ethanol) and electrospinning was done for individual samples.

2.2 Preparation of the polymeric precursor solutions

Granular polyvinyl pyrrolidone (PVP, average molecular weight 40000) purchased from LobaChemie was used as the polymeric component in this study. The polymeric solution was made by dissolving the PVP powder in reagent grade ethanol (Merck, M=46.07 g/mol) under constant and vigorous stirring to give PVP solution. 1.5 g PVP was added to 2.5 ml ethanol and was left under magnetic stirring for thirty minutes until a clear viscous solution of PVP was formed. This concentration was arrived at and selected after several itinerary experimental works with respect to the desired viscosity of the inorganic–organic composite solutions. PVP solutions tended to dry out and leave a stiff gel in the beaker if stored for longer time due to volatile nature of ethanol, a solvent for dissolving PVP. Thus, in order to avoid such circumstances during time of experiment, the PVP solution was prepared only thirty minutes before the electrospinning session.

2.3 Spinning of the fibers

For the electrospinning experiments, equal volumes of the precursor solutions (YSZ and PVP) were added to a beaker and mixed thoroughly in magnetic stirrer until a clear viscous sol was obtained. Both, static and rotating types of collectors were used. A simple collector plate was made by mounting aluminum foil into approximately a 4×4 inch square glass plate. This allowed the fibers to be collected directly onto the aluminum plate. Using the high voltage power supply, 15-20 kV was applied between the needle and the collector plate in order to initiate the electrospinning. The voltage was varied precisely until the fibers began to form steadily and collect on the collector plate facing the syringe, placed about 17.5 cm away from the tip of the needle. Typically, 5 ml of the solution was spun at a time, with a flow rate between 0.2 ml/h. Thus, an individual run lasted about 8 hours every day until a thick layer of fiber was deposited in the collector plate. Every individual run required short interruption time for periodic cleansing of the clogged needle.

2.4 Material Characterization

The as-synthesized zirconia nanofiber was characterized by scanning electron microscopy (SEM), Energy dispersive x-ray spectroscopy (EDS), X-ray diffraction (XRD), and Fourier transform infrared spectroscopy (FTIR).SEM characterization of both as-spun as well as calcinedfibers was performed using JEOL JSM-5300 microscope (acceleration voltage15 kV) and EDS of individual samples were taken at the same time.The X-ray diffraction patterns of the samples were recorded on a Philips Analytical ltd, Holland (PW3040) using Ni-filtered CuKα radiation. The IR spectra of the samples were recorded (as KBr pellets) usingIRPrestige-21 infrared spectrophotometer with a resolution of 4 cm-1, in the range of 400–4000 cm-1 for both as-spun as well as calcinedfiber samples.In this experiment, calcinations of the fiberwere done using a standard tubular furnace with the sample placed in crucible specimen. The crucible after being placed in the tubular furnace was heated at 5^0C/min to the pre-defined temperature ranges and was left for 1 hour (hr) at that particular temperature. Soon after the completion of heating cycle, the furnace was turned off and left to cool overnight. The heating regime used for this experiment is shown as in Figure 1.

2.5 Biological Characterization

2.5.1 MTT Assay

MTT Assay was performed for the in vitro assessment of cytotoxicity caused by as produced zirconia nanofiber. Cell lines (mononuclear cells derived from peripheral blood) cultured in our laboratory were used for this assay. A 96-well round-bottomed microculture plate used for this experiment was incubated with varying concentration of composite zirconia scaffold in presence of cell suspension. Cells co-cultured in absence of any zirconium component were used as a positive control and pure medium is taken as negative control. Plates werethen carefully covered and incubated for 1 and 3 days at 37℃. After 1 day, 50 µg (10 µL of a solution of 5 mg/mL) of MTT (Sigma Aldrich) was added to each well. Plates were

shaken and incubated for another 5 hr at 37 ℃.After exposure of the reagent to the viable cells, yellow MTT was reduced to purple formazan. The formazan crystals were dissolved with 100 µL of dimethylsulfoxide (DMSO) (Fisher Scientific), and the quantity of reduced product was measured by microplatespectrophotometerat 540 nm (Perkin Elmer).The mononuclear cells viability was calculated using the equation (A.1).The optical density (OD)of both control and test wells were adjusted by the ODof blank wells[4].

2.5.2 Haemolysis assay

Approximately 10 ml whole blood was drawn from healthy volunteer using a 5ml disposable syringe. Blood testing solution was prepared by diluting 2 ml fresh EDTA human blood with 5 ml 0.9% saline. Small fraction of zirconia samples calcined at 800^0C and 1100^0C were transferred and equilibrated in 4 ml saline for 30 min at 37^0C.Diluted blood (0.2 ml) was added to each sample and incubated for 60 min at 37^0C. Positive control as Triton X and blood sample without zirconia material as negative control, were performed by adding human blood to distilled water or SBF solution in the ratio of 1:20, respectively. All solutions were centrifuged at 750 × g for 5 min. The optical density (OD) of the supernatant was measured at 545 nm. Haemolysis was calculated as described by Dey and Ray using equation (A.2)[5].In this equation, OD(−) control is the adsorption of 0.2 ml human blood dissolved in 4 ml distilled saline solution; OD(+) control is the adsorption of 0.2 ml human blood dissolved in 4 ml water.

3. Results and Discussion

3.1 Synthesis of YSZ nanofibers

Deposition of nanofibers at different interval of time is shown in Figure 2.fiberwas collected in a horizontal square aluminium collector plate. Appreciable amount of fibers were deposited within 4-5 hours run of the device. Figure 2(e) and (f) represents thick scaffold deposited after electrospinning for 5-6 days (8 hrs per day) continuously. As spun nanofibers collected after several days were about 0.01mm thick.

3.2 Material Characterization of fiber

3.2.1 Characterization by SEM

As compared to 8 YSZ sol (I), there was no any fiber formation during electrospinning of the solution as mentioned in 8 YSZ sol (II). This may be due to the very negligible viscosity of the solutions prepared by this method as compared to the compositions of 8 YSZ sol (I). Viscosity is one of the most important parameter for optimization of electrospinnable properties of any spinning dopes. Lower viscous solution doesn't form any fibers while a solution having very high viscosity often creates difficulty during the process of electrospinning. Optimization of any electrospinnable solution depends upon knowing a critical minimum concentration C_e, the lowest concentration level required for forming beaded nanofibers of that particular solvent-system. Thus, any concentration below C_e fails to yield nanofibers but just droplets[6].

3.2.1.1 Effect of concentration of solution

Diameter of a nanofiber fabricated via electrospinning is closely dependent upon the concentration of the electrospinnable solution. Among four different compositions, one having least PVP concentration (40 wt %) did not reveal any nanofibrous structure during SEM. Formation of droplets at 40 wt% and below solution concentration level is due to the capillary disintegration of the dope by surface tension [11] and also due to low molecular weight liquid [2]. Figure3(a) having PVP concentration as 50 wt% showed deposition of smooth, solid and sparsely distributed nanofibers with numerous bead like structures. The formation of bead-on-string structures can be correlated to the high surface tension and low viscosity of the PVP/YSZ solution. As the concentration of PVP is raised to 60 wt%, Figure3(b) reveals uniformly arranged nanofibers having average diameter in the range of 200 nm and totally devoid of any bead like morphologies. PVP/Ethanol solution possesses a lower tension and higher viscosity due to which more smooth fibers without beads are easily obtained by using the solvent. Morphology of nanofibers fabricated by mixing PVP in ethanol are found to be extremely smooth, diameter as compared to other solvents e.g. N,N-dimethylformamide (DMF), dichloromethane (MC).

Thus, fiber morphology is highly affected by the type of solvents used during electrospinning process[7]. Beside other polymeric precursors, PVP produces abundant electrospun material overcoming use of conventional techniques that has only potential for small-scale ceramic fiber production.Obtaining large fiber diameters at 60 wt% and above concentration, 80 wt% PVP shown in Figure3(c) is a result of increased viscosity. As the viscosity increases, the beads also become bigger moreover the average distance between beads elongates ultimately increasing the fiber diameter and morphology of beads

get changed from spherical to spindle-like. Experimental results, as in Figure 4 shows that the diameter of the nanofibers increases from nanometer scale to micrometer scale with increase in the concentration of PVP in the solution.

3.2.1.2Effect of environmental parameters (Temperature and Humidity)

Two experiments were performed in which both humidity and temperatures were varied. It was observed, as shown in Figure 5 that at higher humidity (>50%), the diameter of the electrospun nano fibers were less as compared to that of lower humidity (30% approx.). This result matches well with the work shown DeVrieze et al [8]. His result also shows that the PVP nanofibers become thinner at higher humidity but stops if crossed beyond a certain upper threshold limit. It was impossible to yield nanofibers when the humidity increased beyond 60-65% when every other parameter was left constant. The rate of evaporation of ethanol doesn't change with varying relative humidity (RH) at the same temperature. The only thing that differs is the absorption of water from the surrounding prolonging the solidification time of nanofiber. Thus, such jet can elongate further and continue longer resulting in the decreased diameter of nanofibers.

The temperature has a significant effect on the average diameter of the PVP nanofibers. At 27^0C, the average diameter of the nanofibers is lesser than at 38^0C as shown in fig [9] but the morphology of fibers at both the temperatures, 27^0C (Figure 3) and 38^0Cisexcellent which can be distinguished from Figure7. This variation in diameter can be correlated with the rate of evaporation of the solvent with the change in temperature. Rate of solvent evaporation decreases exponentially with decreasing temperature thus providing sufficient time for the jet to get solidify prolonging continuation of the jet[8]. Viscosity and solvent evaporation rate are two parameters extremely dependent on the temperature accompanied by influence on the average fiber diameter.

3.2.1.3 Effect of calcinations temperature on fiber morphology

The comparison of YSZ nanofiberscalcined at various temperatures is shown in Figure8. SEMimages of all the fiberscalcined at varying temperature shows presence of intact nanofibers and excellent morphology even after heating at higher temperatures. As compared to the as-spun nanofibers these fibers are also similar in morphology except the variation in diameter of the nanofiber. Only fiberscalcined at 1100^0C shown in Figure8 (g, h) were characterized with few agglomerates and disintegrated morphology. Agglomerates may be due to the coalescence of zirconia nanofibers after complete removal of PVP which might have worked as a template to preserve the intact morphology of as-spun nanofibers in lower temperature variations. Similarly, the broken fiber at this higher temperature may be due to higher amount of solids inside the fibers and the associated shrinkage that increases with the rise in temperature.

The SEM images taken with varying calcinations temperature showed significant reduction in the diameter of the fibers as shown in Figure 9. This reduction in the diameter of calcinednanofibers can be attributed to the burning-off of PVP at higher temperature. The average diameter of fiber obtained after calcination at 1100^0C was 144 nm which is 41% less as compared to as-spun nanofiber. This explains the importance of implementing the optimal heating conditions when electrospun organic/inorganic composite fibers are calcined to get ceramic nanofibers in appropriate quality (morphology) and to avoid their disintegration. When a too high heating temperature is used, the nanofibers are completely disintegrated. When the optimal heating temperatures (300^0C, 600^0C, 800^0C) were applied, intactnanofibers with excellent morphology were obtained.

3.2.1.4 Effect of electric field and cold compression

A simple study was performed to investigate the effect of electric field and cold compression on the morphology of as-spun nanofiber. The variation in electric field by virtue of small metallic conducting pins attached to the aluminium foil altered the fiber deposition mechanism as compared to normal deposition. With this pin attached it was possible to deposit nanofibers oriented mostly in the vicinity of pins with scaffold thickness of approximate 1 mm because the greatest pulling force is exerted on the jet at the point of the needle. In absence of pins the electric field are more likely aligned in parallel fashion towards the entire surface of aluminium foil but after the introduction of a pointed object, a high electric field density exist around the pin.

This type of arrangement help to deposit fiber cluster on the immediate vicinity of pin and the reduction in electric field due to deposition of a thin layer of fiber is counter balanced by the high electric field density. It can now be settled that changing the setup from a grounded plate to a grounded needle has a significant effect on the electrostatic field and indicates that the spun fiber will unite towards this point and thus improved thickness of nanofibrous mat can be easily obtained with a slight modification in the type of collector [4]. The SEM analysis of fibers after cold compression for 1

hour in liquid nitrogen revealed no significant changes in the morphology of fibers as compared to fibers without it. The intact fiber morphology can still be observed in such scaffolds, Figure 10 even though treated at very low temperatures.

3.2.2Analysis by EDS

The energy dispersive spectrum (EDS) in Figure 11 clearly shows the presence of Zirconia,Yttria, Oxygen as an elemental component of calcinedfiber. Thus it can be proved that the final product after calcinations consists only of expected compound and is completely pure in nature.

3.2.3Characterization by XRD

The formation of ceramic fibers solely depends upon the transition from its precursor to ceramic materials after applying proper heat treatment technique. The XRD curves shown in Figure 12 for both as-spun and calcinedfiber samples reveals cubic phase of YSZ fibers with an average grain size varying from 4 nm to 47 nm with the increase in calcinations temperature respectively.

The curve corresponds to the amorphous phase of as-spun PVP/YSZ composite fibers at room temperature and semi crystalline at 300^0C. Few very indistinct peaks at this temperature seem to be an outcome of semi crystalline nature of YSZ fibers at 300^0C. Notably, after the calcination of PVP/YSZ composite above 300^0C, amorphous phase of PVP/YSZ disappeared, and various reflection peaks at 29.96, 34.7, 49.92, 59.32 corresponding to the pure ZrO_2 crystalline with cubic phase of YSZ appeared. This result matches well with the cubic phase zirconia (JCPDS cards: No. 30-1468) that is available in literature[9]. The average crystal size of the zirconia nanofibers obtained at different calcinations temperature was approximated by the Scherrer method using equation (A.3).The peaks of 8YSZ crystal became sharper and narrow as shown in Figure13, with increasing calcination temperature to 1100^0C, which indicated that the crystallinity was higher and the grain size was larger at high calcination temperature than those obtained at low calcinations temperature.

3.2.4Characterization by FTIR:

Five different ZrO_2 samples spectra including as-spun and calcined samples at 300, 600, 800 and 1100^0C were obtained. Characteristic spectra for the different samples are presented in Figure 14 to illustrate its remarkable features. The spectrum of the as-prepared amorphous ZrO_2stabilised by the addition of 8 mol% yttria is shown in Figure 14(a). The broad band in the 3500 cm^{-1} region may be attributed for the retention of atmospheric moisture as well as due to OH^- groups from the starting material. The band in 1380 cm^{-1} region was found to be distinct in as-spun sample but not all, of the samples examined. Broad band in this region are commonly distinct in spectra of metal oxides due to adsorbed CO_2[10] that may vary with respect to temperature and crystal structure of the oxide. Hence, similar bands in the spectra of ZrO_2 are attributed to impurities formed from adsorbed atmospheric CO_2.

The other spectra of significant interest in the as-spun sample are in the region of 1637 cm^{-1}. This band is attributed for the adsorption of PVP in the sample before calcinations. However these bands were significantly reduced with the increase in calcinations temperature and were not observed in the fibers after calcined at 1100^0C. Thischange in the spectra highly convinces that the thermal treatment was quite effective in removing PVP after calcinations at higher temperatures. Moreover, IR spectra of sample calcined at 1100^0C shown in Figure 14 are completely devoid of any impurities as compared to other samples at lower temperature.

The IR spectra on its lower frequency side, Figure 14 (f) are significant outcome of this investigation. It can be clearly observed that the IR spectra band at 418 and 667 cm^{-1} is weak and hardly visible in the sample before calcinations. The incipient weak band on its lower frequency side was better developed with the increase in calcinations temperature. A sharp peak that can be easily distinguished in the samples after calcinations at 300, 600, 800 and 1100^0C in the range of 418 cm^{-1} and 667 cm^{-1} corresponds to the absorption of Zr-O bond. Thus, this result clearly indicates the existence of ZrO_2 after applying proper heat treatment at varying temperature. It may be noted that beside several obvious bands due to C-H, C=O, C-N interactions in the obtained spectrum of different samples, only bands of significant interest are taken into consideration in the entire description of IR spectroscopy.

3.3Biological Characterization of fibers

3.3.1 MTT Assay

In this experiment, the result of the MTT assay in Figure 15 showed slight difference between 800 and 1100^0C calcined sample palettes for both day 1 and 3. The chemical activity of cells grown on zirconia palettes calcined at 1100^0C materials

was remarkably higher than those on 800^0C, indicating that materials calcined at higher temperature were more encouraging to cell proliferation than the lower one. Hence, it can easily be understood that as-prepared zirconia is a completely biocompatible material.

3.3.2 Haemolytic Assay

The haemolysis values for the two zirconia samples calcined at 800^0C and 1100^0C are shown in Figure 16. Haemolysis was less than 1% for all tested materials. This fits quite well within the tolerable boundary set by Autian, who reported that a value of up to 5% haemolysis is acceptable for biomaterials[11]. No significant difference was observed between zirconia fiberscalcined at different temperature, yet the value of haemolysis on sample calcined at 1100^0C was slightly greater than the sample calcined at 800^0C. This test has been approximately conducted within minimum delay of 2 hours which ensures that the blood properties haven't changed during entire experimental hours. Hence, this result clearly shows that as prepared scaffold has least haemolytic effect.

4. Conclusion

This paper describes simple method for the preparation of polycer derived 8 mol% YSZ zirconianano fibers having diameter of ~200 nm by the technique of electrospinning. Optimization of yttria stabilized zirconia electrospinnable dope that could yield minimum fiber diameter and excellent morphological features was completed successfully after several iternary experimental work outs. The polymer concentration, temperature and humidity had significant effect in the morphology and electrospinnability process of YSZ ceramic nanofibers. Unlike other polymeric precursors, PVP (60 wt %) produced abundant electrospun material overcoming use of conventional techniques that has only potential for small-scale ceramic fiber production. Moderate atmospheric temperature and slightly higher humid environment strongly favours electrospinning process to obtain high quality ceramic nanofibers.

The XRD curves showed that the as-prepared scaffold were pure crystalline ZrO_2 nanofibers having amorphous phase while in room temperature but transformed to cubic phase with an average grain size varying from 4 to 47 nm when the temperature was raised above 300^0C. Here, 8mol% yttria helped to "lock" the cubic phase of zirconia even in the room temperature and yield ceramic fibers possessing exceptional properties. Results obtained from FTIR and EDX also clearly indicated the existence of ZrO_2 after applying proper heat treatment at varying temperature.

A simple study was performed to investigate the effect of electric field and cold compression on the morphology of as-spun nanofiber. The variation in electric field by virtue of small metallic conducting pins attached to the aluminium foil confirmed possibility to fabricate thick scaffolds of nearly 1 mm thickness having uniform fiber morphology.

Biological characterization of 8 YSZ fibers performed using MTT assay indicated that materials calcined at higher temperature (1100^0C) were more encouraging to cell proliferation than the lower one (800^0C) and haemolysis was less than 1% for all materials tested by haemolytic assay. Hence, it can be concluded that 8 YSZ fibers fabricated by this technique is a completely biocompatible material and has least haemolytic effect enhancing its further in vivo use in the biomedical areas.

References

[1]. Li D, Xia Y. Electrospinning of Nanofibers: Reinventing the Wheel? Advanced Materials 2004;16:1151-70.
[2]. Grant CD, Schwartzberg AM, Smestad GP, Kowalik J, Tolbert LM, Zhang JZ. Characterization of nanocrystalline and thin film TiO2 solar cells with poly(3-undecyl-2,2′-bithiophene) as a sensitizer and hole conductor. Journal of Electroanalytical Chemistry 2002;522:40-8.
[3]. Dai Y, Liu W, Formo E, Sun Y, Xia Y. Ceramic nanofibers fabricated by electrospinning and their applications in catalysis, environmental science, and energy technology. Polymers for Advanced Technologies 2011;22:326-38.
[4]. Solberg RHM. Position-controlled deposition for electrospinning: Eindhoven University of Technology; 2007.
[5]. RAO BVSS. High Performance Ceramics. Delhi, India: Mohan Primlani for Oxford and IBH Publishing Co. Pvt. Ltd.; 1987.
[6]. Luo CJ, Nangrejo M, Edirisinghe M. A novel method of selecting solvents for polymer electrospinning. Polymer 2010;51:1654-62.
[7]. Yang Q, Li Z, Hong Y, Zhao Y, Qiu S, Wang C, et al. Influence of solvents on the formation of ultrathin uniform poly(vinyl pyrrolidone) nanofibers with electrospinning. Journal of Polymer Science Part B: Polymer Physics 2004;42:3721-6.
[8]. De Vrieze S, Van Camp T, Nelvig A, Hagström B, Westbroek P, De Clerck K. The effect of temperature and humidity on electrospinning. Journal of Materials Science 2009;44:1357-62.
[9]. Azad A-M. Fabrication of yttria-stabilized zirconia nanofibers by electrospinning. Materials Letters 2006;60:67-72.

[10]. Phillippi CM, Mazdiyasni KS. Infrared and Raman Spectra of Zirconia Polymorphs. Journal of the American Ceramic Society 1971;54:254-8.
[11]. Qu X-H, Wu Q, Chen G-Q. In vitro study on hemocompatibility and cytocompatibility of poly(3-hydroxybutyrate-co-3-hydroxyhexanoate). Journal of Biomaterials Science, Polymer Edition 2006;17:1107-21.

Appendices

Formulae and Equations

Eq. (A.1)Cell Viability = (OD of Zirconia exposed well/Mean OD of control wells)× 100%

Eq. (A.2)Haemolysis = [OD of Test sample – OD (-) control] / [OD (+) control – OD (-) control] ×100

Eq. (A.3) $D = 0.89\lambda/\beta \cos\theta$

where,

D=crystallite size (grain diameter)

λ=wavelength of the X-ray radiation (CuKα1=0.15418nm)

β=broadening of diffraction line measured as half of its maximum intensity,

θ=corresponding angle

The full width at half maxima (β) (FWHM)of the corresponding peaks was calculatedby Gausspeak fitting tool in Origin software 8.6 version.

List of Figures

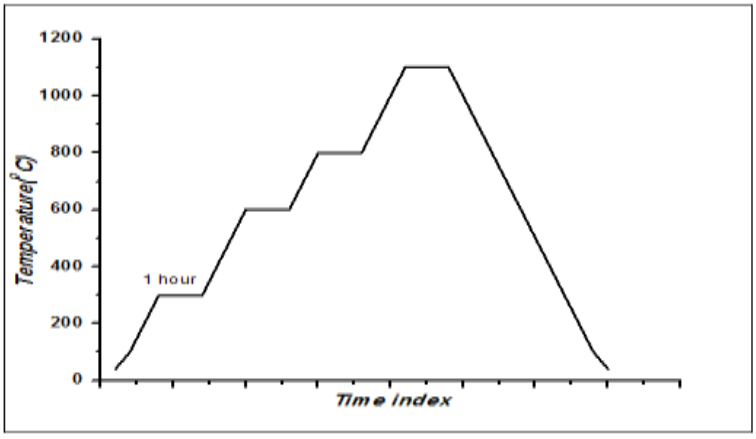

Figure 1: Heating regime used for Calcination of samples

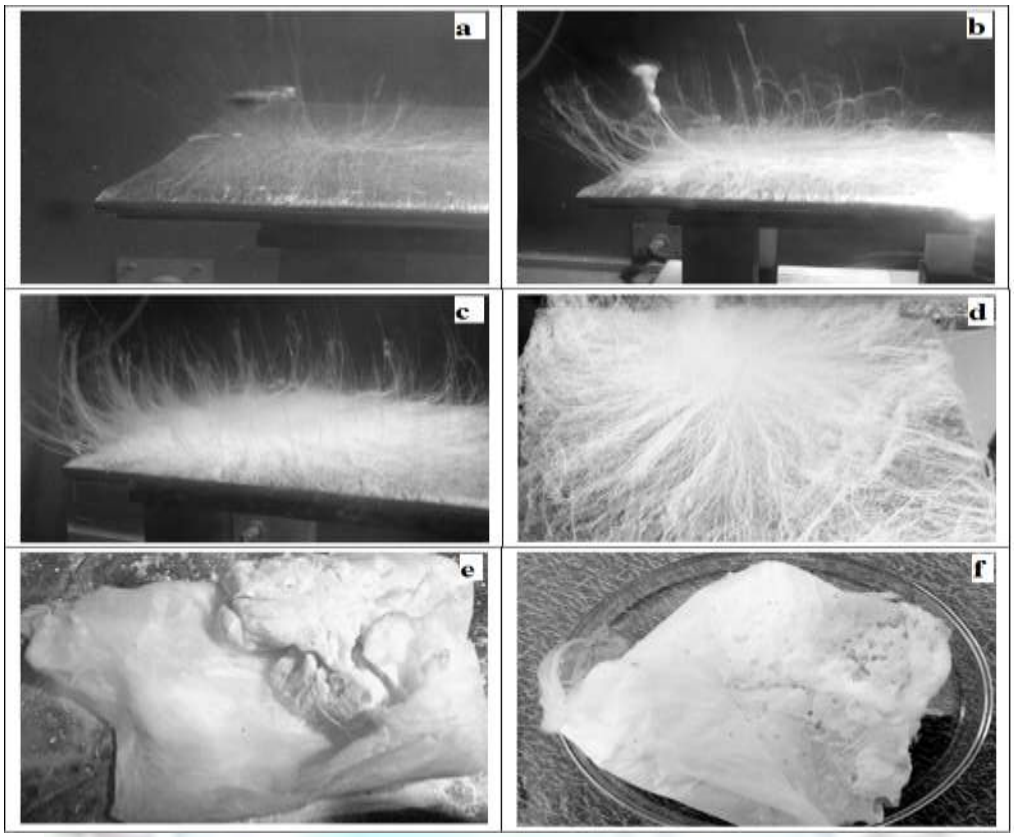

Figure 2:Deposition of 8 mol% YSZ fibers at different interval of time; images taken after (a) 5, (b) 15, (c) 25, (d) 60 min, (e)and (f) 48 hrs from the starting of process.

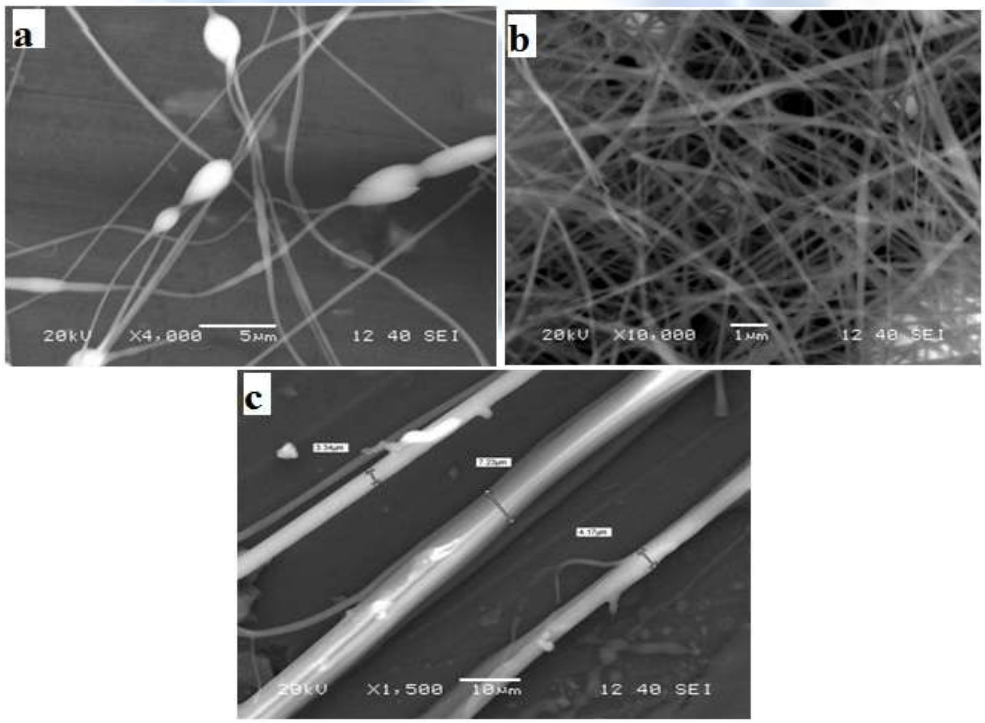

Figure 3: SEM images of fiberselectrospun at various PVP concentrations: (a) PVP 50 wt%, (b) 60 wt% and (c) 80 wt%

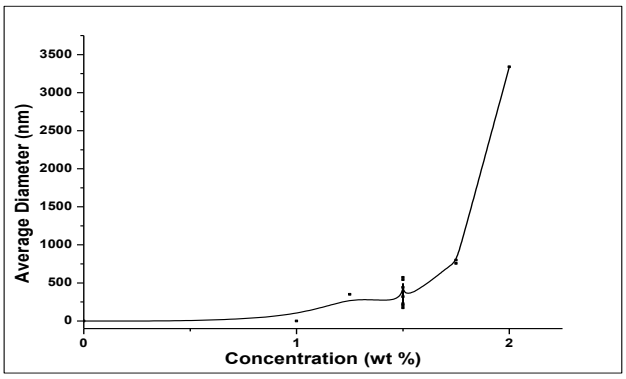

Figure 4: Effect of varying concentration in fiber diameter

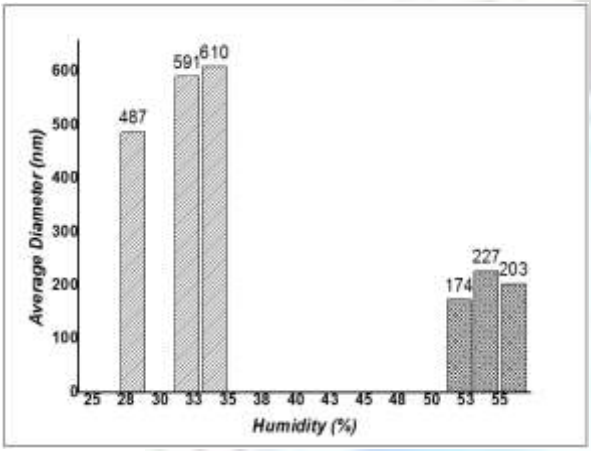

Figure 5: Effect of humidity in fiber diameter

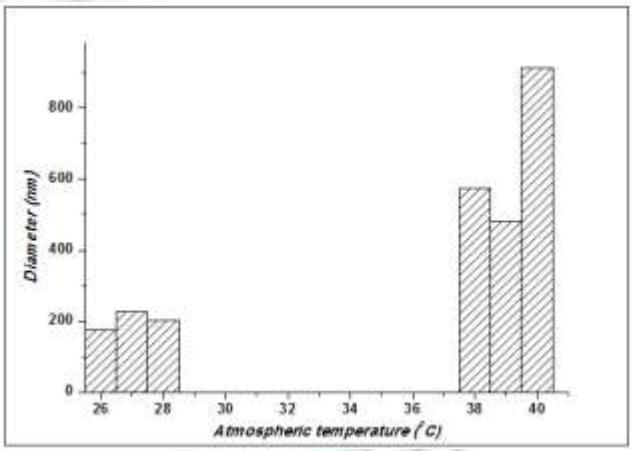

Figure 6: Effect of atmospheric temperature in fiber diameter

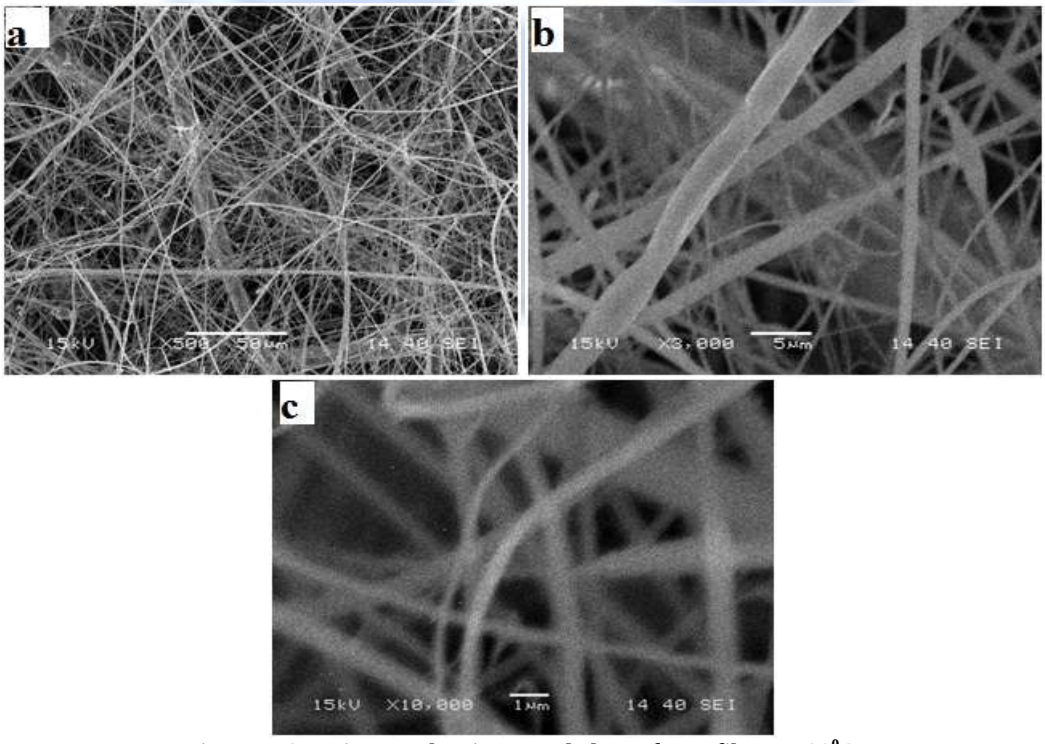

Figure 7: SEM images showing morphology of nanofibers at 38^0C

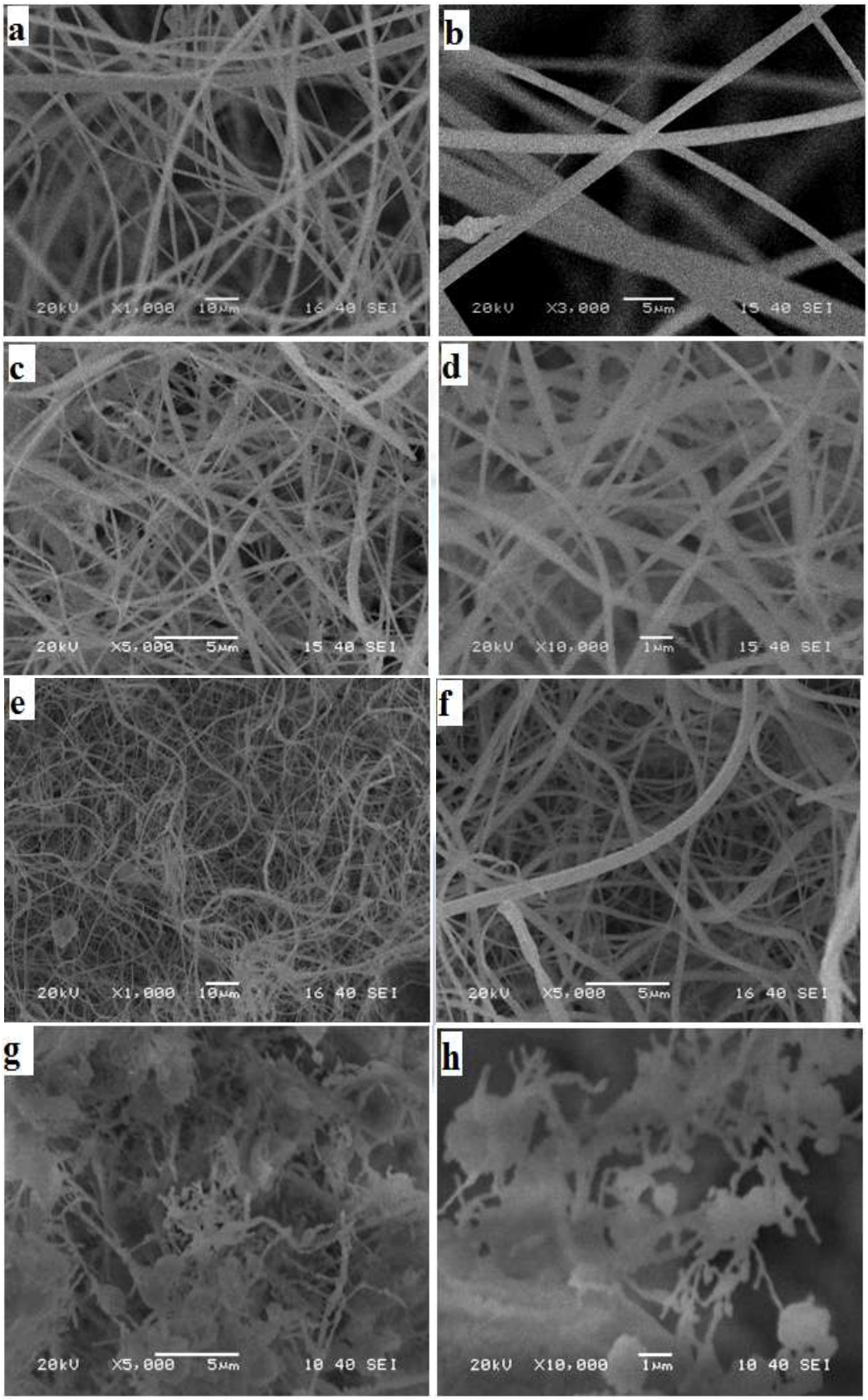

Figure 8: SEM images of fibersafter calcinations at; 300 (a, b), 600 (c, d), 800 (e, f) and 1100^{0}C (g, h).

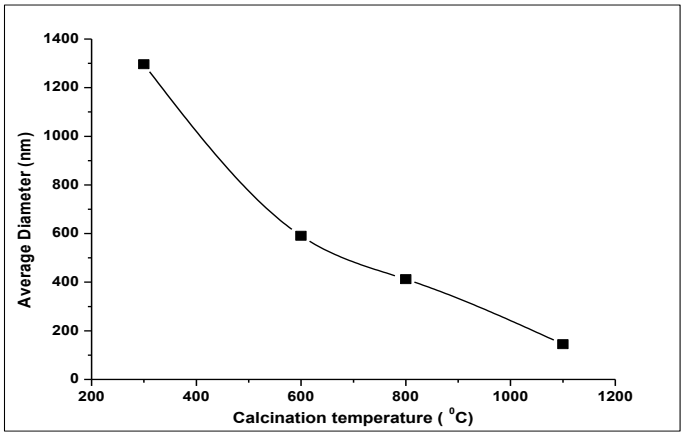

Figure 9: Effect of calcination temperature in fiber diameter

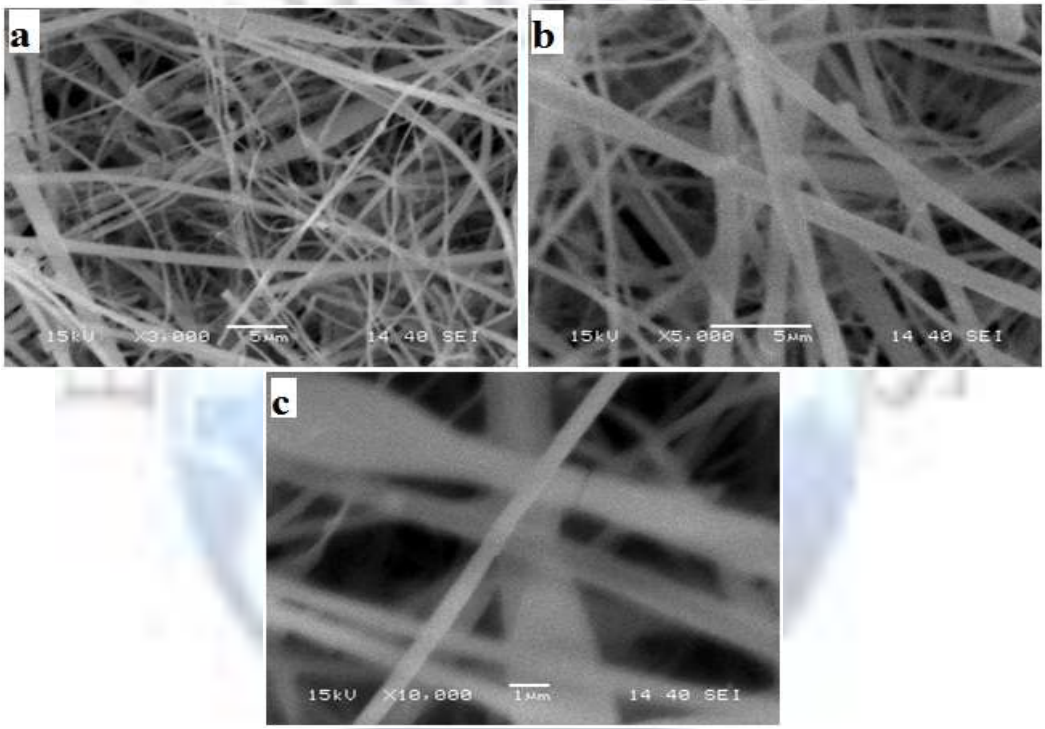

Figure 10: Effect of cold compression in fibers morphology

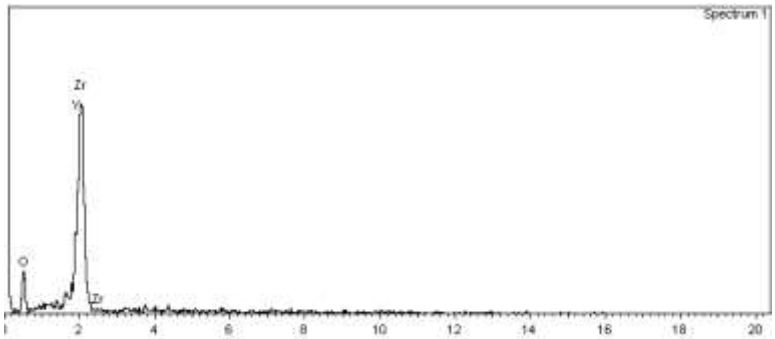

Figure 11: EDS image showing approximate elemental composition of fibers after calcination

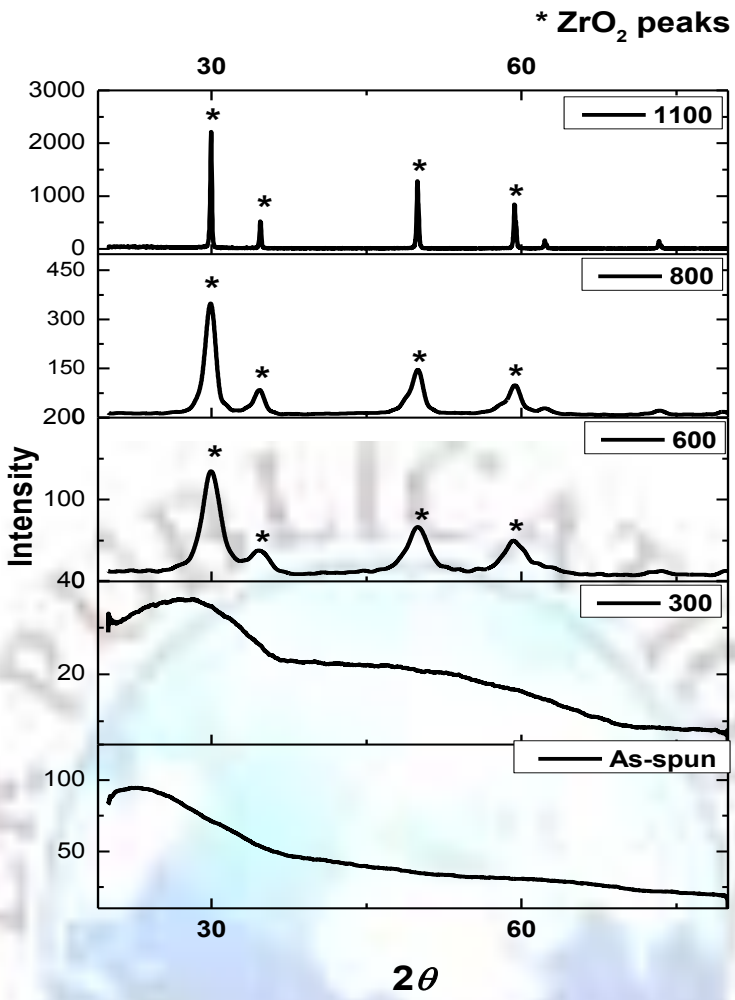

Figure 12: XRD curves of fibers before and after calcinations

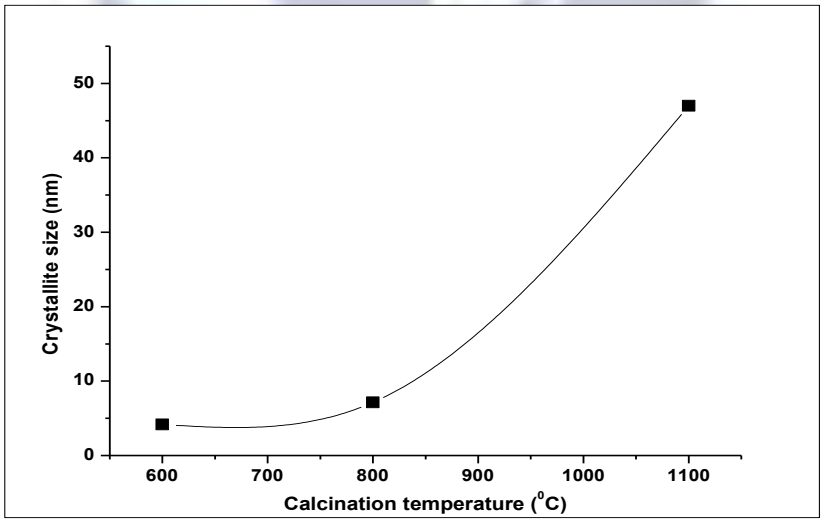

Figure 13: Effect of Calcination on crystallite size

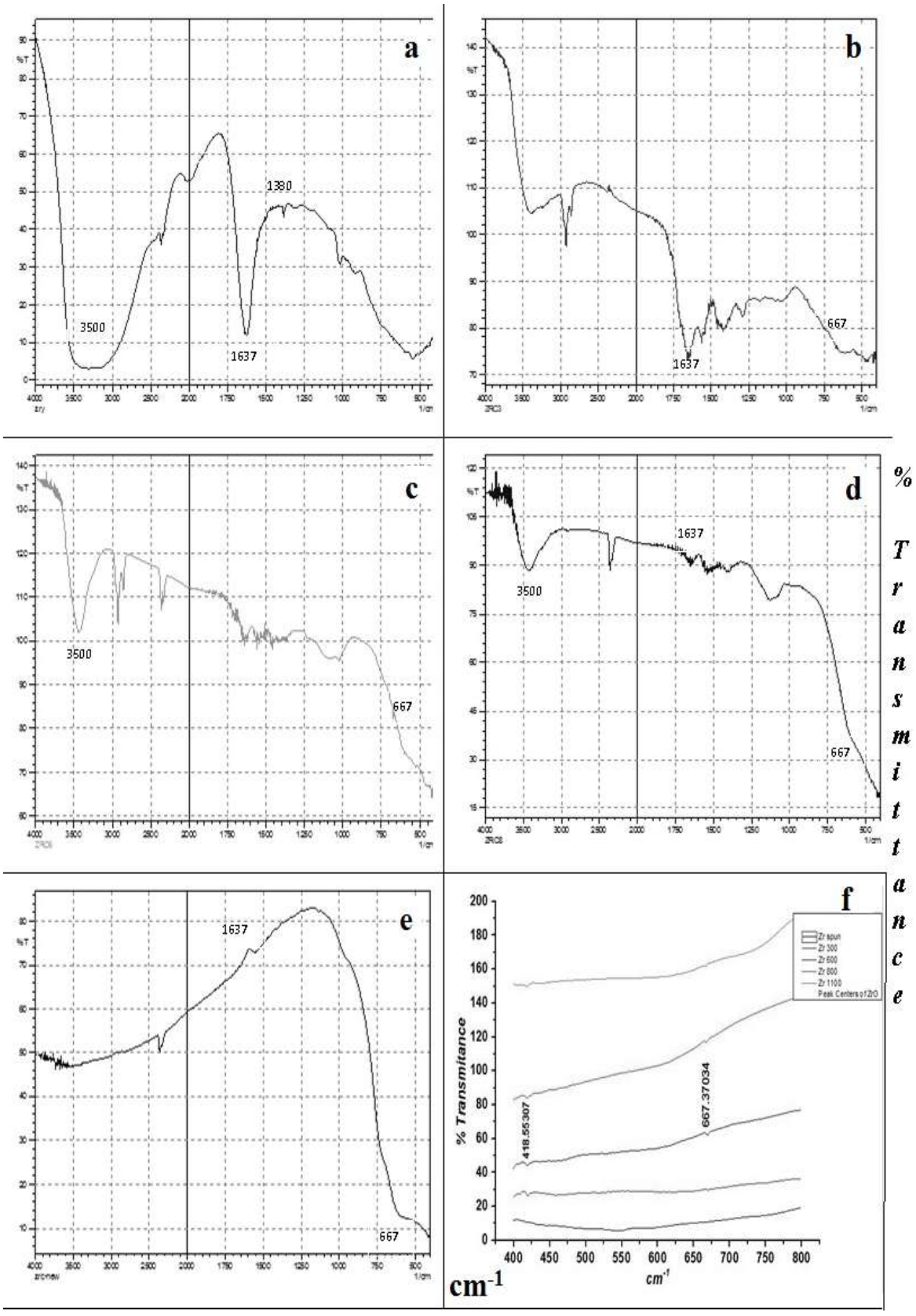

Figure 14: FTIR spectra of samples before and after calcination; as-spun (a), 300 (b), 600 (c), 800 (d), 1100^{0}C and expanded lower range (400-800 cm-1) of all samples (f)

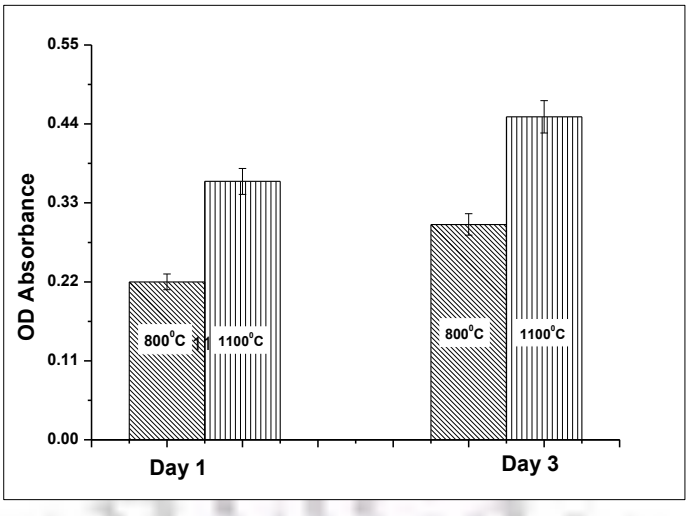

Figure 15: MTT assay results of 8 mol% YSZ samples calcined at 800 and 1100^{0}C for day 1 and 3

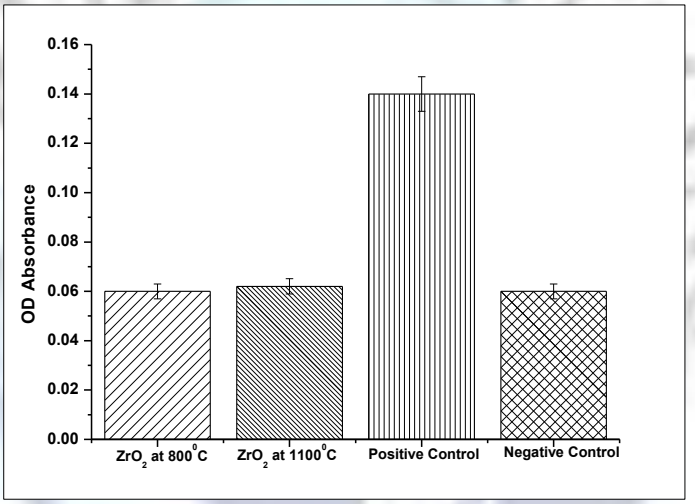

Figure 16: Haemolytic assay results for samples calcined at 800 and 1100^{0}C